IEEE Access
Multidisciplinary | Rapid Review | Open Access Journal

Received August 8, 2019, accepted August 25, 2019, date of publication August 29, 2019, date of current version September 13, 2019.

Digital Object Identifier 10.1109/ACCESS.2019.2938402

An Automated and Accurate Spine Curve Analysis System

BO CHEN[1], QIUHAO XU[2], LIANSHENG WANG[2], STEPHANIE LEUNG[3], JONATHAN CHUNG[3], AND SHUO LI[1], (Member, IEEE)

[1]Digital Imaging Group of London, Department of Medical Imaging, Western University, London, ON N6A 4V2, Canada
[2]Department of Computer Science, Xiamen University, Xiamen 361005, China
[3]Department of Medical Imaging, Western University, London, ON N6A 4V2, Canada

Corresponding authors: Liansheng Wang (lswang@xmu.edu.cn) and Shuo Li (slishuo@gmail.com)

ABSTRACT We present a new Adaptive Error Correction Net (AEC-Net) to formulate the estimation of Cobb anges from spinal X-rays as a high-precision regression task. Our AEC-Net introduces two novel innovations. (1) The AEC-Net contains two networks calculating landmarks and Cobb angles separately, which robustly solve the disadvantage of ambiguity in X-rays since these networks focus on more features. It effectively handles the nonlinear relationship between input images and quantitative outputs, while explicitly capturing the intrinsic features of input images. (2) Based on the two estimated angles, the AEC-Net proposed a new loss function to calculate the final Cobb angles. The optimization of the loss function is based on a high-precision calculation method. The deep learning structure is used to complete this optimization, which achieves higher accuracy and efficiency. We validate our method with the spinal X-rays dataset of 581 subjects with signs of scoliosis at varying extents. The proposed method achieves high accuracy and robustness on the Cobb angle estimations. Comparing to the exsiting conventional methods suffering from tremendous variability and low reliability caused by high ambiguity and variability around boundaries of the vertebrae, the AEC-Net obtain Cobb angles accurately and robustly, which indicates its great potential in clinical use. The highly accurate Cobb angles produced by our framework can be used by clinicians for comprehensive scoliosis assessment, and possibly be further extended to other clinical applications.

INDEX TERMS AEC-Net, Cobb angle estimation, deep learning, direct estimation, high-precision calculation.

I. INTRODUCTION

Cobb angles are widely used for scoliosis diagnosis and treatment decisions. Scoliosis is a structural, lateral, rotated curvature of the spine, which especially arises in children at or around puberty and leads to disability [1]. For clinical examination of scoliosis, the radiography (X-ray) is the most common imaging technique with cheap acquisition and less time cost [2]. Cobb angles derived from a posteroanterior (back to front) X-ray and measured by selecting the most tilted vertebra at the top and bottom of the spine with respect to the horizontal line are typically used to quantify the magnitude of spinal deformities [3].

However, conventional landmark-based manual measurement [4], [5] involves the indirect calculation of identifying the vertebrae and measuring angles, which suffers from high inter- and intra-observer variability while being time-consuming. The accuracy of Cobb angles is often affected by many factors such as the selection of vertebrae, the bias of observer, the accuracy of landmark measurement, as well as image quality. These variabilities in measurements can affect diagnosis significantly when assessing scoliosis progression. Moreover, it is also challenging to estimate Cobb angles automatically due to the high ambiguity and variability of X-rays. As shown in Fig. 1, large anatomical variability and low tissue contrast can lead to complex identification of interesting vertebrae and further measurement. It is therefore important to provide accurate and robust quantitative measurements for Cobb angles.

The associate editor coordinating the review of this article and approving it for publication was Aysegul Ucar.

A. PREVIOUS METHODS

1) SEGMENTATION AND FILTER BASED METHODS

Methods proposed in the literature such as Active Contour Model [4], Customized Filter [5] and Charged-Particle Models [6] were used to localize the required vertebrae in order

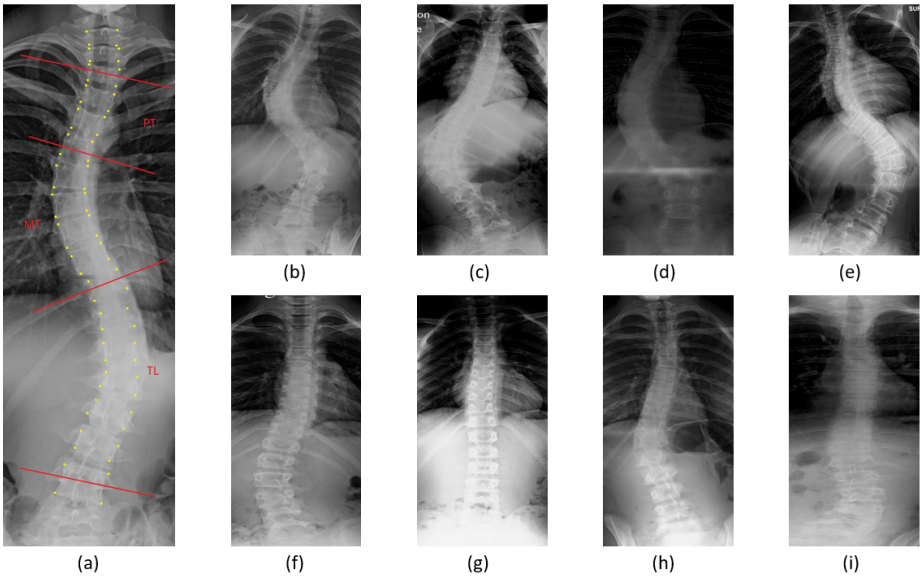

FIGURE 1. Traditional methods use landmark (yellow points in (a)) to measure cobb angles (a). It is challenging to measure three cobb angles: Proximal-thoracic (PT), main thoracic (MT), thoracic-lumbar (TL) due to high ambiguity and variability in scoliosis X-rays from different subjects (a-i).

to derive the Cobb angle from their slopes. These methods require accurate vertebrae segmentations and feature engineering, which makes them computationally expensive and susceptible to errors caused by variation in X-ray images.

2) MACHINE LEARNING BASED METHOD

Machine learning algorithms such as Support Vector Regression (SVR) [7] and the BoostNet [8] have been used for landmark estimation. Although these methods obtained effective performance, there are still some limitations exist when we apply them for Cobb angle estimation: (1) These methods require high quality images of the spine for landmark coordinates detection, and then use the landmark to calculate the Cobb angles. Hence, these methods would not work well with noising images. (2) These methods rely on the landmark coordinates to calculate the angle, and they perform worse on the angles than they work on the landmark coordinates since a small error in landmark coordinates may cause a big error in the angle.

3) DIRECT METHODS

To circumvent these limitations, direct methods [9]–[15] were proposed to roughly estimate Cobb angles. Two initial attempts [8], [16] have been put forward in conference. Sun *et al.* [16] aimed to improve the robustness of spinal curvature assessment by consolidating the tasks of vertebral landmark detection with Cobb angle estimation by exploiting the dependency between the two tasks. Wu *et al.* [8] achieved robust spinal landmark estimation by automatically removing deleterious outlier features on x-rays images. Despite their effectiveness in landmark estimations, these methods didn't achieve high accuracy in Cobb angle estimation.

4) HIGH-PRECISION CALCULATION

High-precision calculation, a catalog of methods in numerical mathematics, can be used to achieve complex calculation with high accuracy, and to calculate complex expression numerically. The extrapolation [17] is one of the most useful methods in the high-precision calculation. Mathematically, the extrapolation provides a combination function of the functional value at measured data to speculate the functional value, which makes the estimated value much more close to the ground truth. To achieve higher accuracy, the combination function depends on a series of rough measured data. However, it is very time consuming to calculate the parameters of the combination function. Deep learning (DL) structure can effectively solve this problem by automatically and adaptively learning these parameters since it is much less time consuming using numeral approximation instead of complex precise calculation.

B. PROPOSED METHOD

In this paper, we propose an Adaptive Error Correction Net (AEC-Net) to calculate the Cobb angles directly. The AEC-Net firstly estimates Cobb angles using two methods. (a Landmark Net for regressing landmarks, that are used to calculate Cobb angles indirectly; and an Angle Net for regressing Cobb angles directly.) Then it employs an alternative error correction Net using extrapolation to adaptively offset the errors of the two estimated Cobb angles by each other, and obtain an enhanced estimation. The high-precision calculation applied in this work is for decreasing error. Incorporating in a DL structure, the alternative error correction Net learns a combination of the two Cobb angles estimations adaptively solving the approximation equation iteratively,

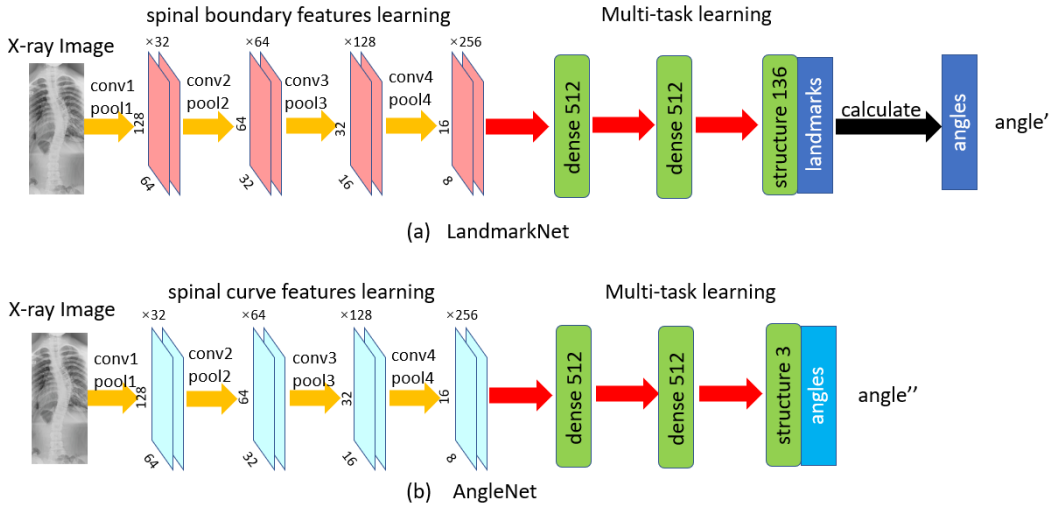

FIGURE 2. Schemes of landmark net (a) for indirect angle estimation and angle net (b) for direct angle estimation.

which further improves the accuracy and effectiveness of the calculation. Therefore, AEC-Net can obtain a more accurate estimation.

C. CONTRIBUTION

Our work contributes in three aspects: (1) A highly accurate and robust clinical Cobb angle measurement is achieved to help physicians to avoid tedious work and reduce inter- and intra-observability; (2) For the first time, high-precision calculation, a powerful numerical method is integrated into a deep learning frame-work; (3) The newly proposed two-stage optimization provides efficient optimization to achieve both fast convergence and high accuracy.

II. METHODOLOGY

Our AEC-Net consists of three parts: (1) A Landmark Net for spinal boundary features learning to regress the landmarks, which are used to calculate Cobb angles ($angle'$) indirectly. (2) An Angle Net for spine curve features learning to regress the Cobb angles ($angle''$) directly. (3) An alternative error correction Net for leveraging both angle estimations through a specially designed combination function using extrapolation to combine the error complementarity between the two estimates. The AEC-NET uses two estimates from the Landmark Net and Angle Net as a reference, and then uses the alternative error correction Net to learn a combination function of these references to improve the accuracy of the final results.

A. LANDMARK NET FOR INDIRECT ANGLE ESTIMATION

As shown in Fig. 2(a), Landmark Net is designed to learn the spinal boundary features in order to obtain robust spinal landmarks for comprehensive scoliosis assessment, and use those landmarks for indirect Cobb angle calculation. It consists of two convolution net parts: (1) Spinal boundary features learning: a large convolution kernel is used to capture large gray level differences around pixels (especially for blurred images and unclear boundary) for learning the spinal boundary features, and (2) Multi-task learning: a dedicated landmarks estimator network that uses these spinal boundary features to regress landmarks. The construction of the Landmark Net is shown in Table 1.

TABLE 1. Construction of the landmark net. Learn the landmark and calculate the angle using landmark.

Name	Kernel Size	Stride	Pad	Output Size
input	-	-	-	256×128×1
conv1	7×7	1	3	256×128×32
relu1	-	-	-	256×128×32
pool1	2×2	2	0	128×64×32
conv2	3×3	1	1	128×64×64
relu2	-	-	-	128×64×64
pool2	2×2	2	0	64×32×64
conv3	3×3	1	1	64×32×128
relu3	-	-	-	64×32×128
pool3	2×2	2	0	32×16×128
conv4	5×5	1	2	32×16×256
relu4	-	-	-	32×16×256
pool4	2×2	2	0	16×8×256
fc1	1×1	1	0	1×1×512
relu5	-	-	-	1×1×512
fc2	1×1	1	0	1×1×512
relu6	-	-	-	1×1×512
fc3/output	1×1	1	0	1×1×136

To better leverage the spinal boundary features and the regressed landmarks, the Landmark Net here uses a loss function:

$$Loss_{Landmark\ Net} = Loss_{landmark\ error} + \lambda_1 Loss_{boundary} \quad (1)$$

TABLE 2. Construction of the angle net. Learn the angle directly.

Name	Kernel Size	Stride	Pad	Output Size
input	-	-	-	256×128×1
conv1	5×5	1	2	256×128×32
relu1	-	-	-	256×128×32
pool1	2×2	2	0	128×64×32
conv2	3×3	1	1	128×64×64
relu2	-	-	-	128×64×64
pool2	2×2	2	0	64×32×64
conv3	3×3	1	1	64×32×128
relu3	-	-	-	64×32×128
pool3	2×2	2	0	32×16×128
conv4	5×5	1	2	32×16×256
relu4	-	-	-	32×16×256
pool4	2×2	2	0	16×8×256
fc1	1×1	1	0	1×1×512
relu5	-	-	-	1×1×512
fc2	1×1	1	0	1×1×512
relu6	-	-	-	1×1×512
fc3/output	1×1	1	0	1×1×3

The mean square error (MSE) between ground thruth and the predict landmarks, $Loss_{landmark\ error}$, is used in Landmark Net to evaluate the results of multi-task learing. Since the landmark ground truth is the intersection of the vertebra's boundary, which contains the essential information of spine curve features for Cobb angle detection, the Landmark Net uses Pearson Correlation Coefficient to evaluate the boundary features learning results, $Loss_{boundary}$. λ_1 in Eq. 1, is a weight, which is selected based on our experiments. It is set to be 1, and a constraint is added to force the losses of boudary feature learning to be no larger that those of landmark errors. The starting learning rate of the Landmark Net was 0.0005, after every 200 epochs it was divided by 2. It had 3000 epochs in total.

B. ANGLE NET FOR DIRECT ANGLE ESTIMATION

As shown in Fig. 2(b), Angle Net is designed to learn the spinal curve features in order to estimate the Cobb angles directly. It consists of two convolution net parts: (1) Spine curve features learning: a small convolution kernel is used to capture little gray level differences near pixels for learning the spinal curve features, which accumulate region curve information to global curve information, and (2) Multi-task learning: a dedicated Cobb angles estimator network that uses the spine curve features to regress Cobb angles. The construction of the Angle Net is detailed in table 2.

The Angle Net uses a loss function:

$$Loss_{Angle\ Net} = Loss_{angle\ error} + \lambda_2 Loss_{spine\ curve} \quad (2)$$

It uses log of hyperbolic cosine to minimize the error between ground truth and the predict angles, $Loss_{angle\ error}$, Since the relationship between the error of angles and pixels is not linear. Moreover, the angle ground truth reflects the accumulation of the spinal curve, which plays a significant role in spine curve features. The Angle Net uses Pearson Correlation Coefficient to evaluate the spine curve multi-task learning results, $Loss_{spine\ curve}$. λ_2 in Eq. 2, is a weight, which is selected based on our experiments. It is set to be 1, and a constraint is added to force the losses of spine curve multi-task learning to be no larger that those of angle errors. The starting learning rate of Angle Net was also 0.0005, after every 200 epochs it was divided by 2. It had 3000 epochs in total.

C. ALTERNATIVE ERROR CORRECTION NET FOR ACCURACY IMPROVEMENT

The alternative error correction Net is designed to further improve the accuracy of the estimations based on the Landmark Net and Angle Net. We are given the ground truth $angle_0$ and two input angles from Landmark Net and Angle Net.

$$angle_0 = (PT_0, MT_0, TL_0) \quad (3)$$
$$angle' = (PT', MT', TL') \quad (4)$$
$$angle'' = (PT'', MT'', TL'') \quad (5)$$

Here PT (Proximal-Thoracic), MT (Main Thoracic), and TL (Thoracic-Lumbar) are three Cobb angles using in scoliosis assessment. The aim of the alternative error correction Net is to generate our estimation $angle_{est}$, an approximation of $angle_0$, using $angle'$ and $angle''$.

1) SCHEMES OF ALTERNATIVE ERROR CORRECTION NET

As shown in Fig. 3 and Algorithm 1, the alternative error correction Net (1) normalizes the angle sequence as norm-angle, optimize the norm-angle's error to decrease global error, and (2) optimizes the norm-angle to learn the optimal descent direction. The alternative error correction Net accomplishes these process by using the iterative angle training algorithm (IAT).

Algorithm 1 Iterative Angle Training

1: Set initial of angle sequence $angle[0] = (angle', angle'')$
2: **repeat**
3: calculate $angle_{norm}$ using Eq. 8
4: update $angel_{est}$ using $angle_{norm}$
5: calculate $angle_{cor}$ using Eq. 20
6: update $angle[n]$ using $angle^{(i)} = angle_{cor}, i = 1 or 2$
7: **until Convergence**

The iterative angle training algorithm leverage the similarities between tasks of the norm-angle estimator (Eq. 8) and angle sequence estimator (Eq. 10) for accelerating the convergence. To accomplish this, the two estimations of Cobb angles are used to train the alternative error correction Net through Stochastic Gradient Descent optimization. A two-stage alternating optimization scheme was used to

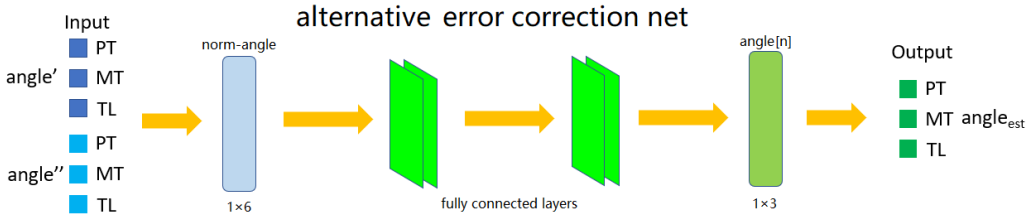

FIGURE 3. The alternative error correction net. The alternative error correction Net iteratively optimize the ref-angle and norm-angle to learn the optimization direction and step length, which can obtain a more accurate estimation.

train norm-angle estimator and angle sequence estimator of the alternative error correction Net iteratively to ensure a synergistic effect when optimizing the two related tasks (Fig. 4).

We optimized the norm-angle estimator and angle sequence estimator alternately (one after the other). The joint optimization scheme allows the Alternative error correction Net to leverage the reciprocal relationship between norm-angle and angle sequence for more fast and accurate Cobb angle estimation (since angle sequence can be computed using norm-angle). The general outline of the iterative 2-stage training scheme is summarized in Algorithm 1. Where $n = 481$ is the number of training data, each training data includes the final three Cobb angles.

The loss function of alternative error correction Net is

$$Loss = \underbrace{\|angle_{cor} - angle_0\|_2^2}_{\text{angle sequence estimation}} + \lambda \underbrace{\|angle_{est} - angle_0\|_2^2}_{\text{norm-angle estimation}} \tag{6}$$

The starting learning rate of alternative error correction Net was 0.0006. It had 10000 epochs totally. We trained the networks using AdamOptimizer. The models and training algorithm was implemented in Python 2.7 using Tensorflow.

2) COMBINATION FUNCTION

We choose the following combination function:

$$\mu angle' + \nu angle'' \tag{7}$$

The μ, ν are extended to real numbers. Weigthed averages $\mu = \nu = 1/2 or \nu = 1 - \mu$ $(0 \leq \mu \leq 1)$, generally have two limitations: 1) when $angle'$ and $angle''$ are greater than or less than $angle_0$ at the same time, it's inevitable the error of weighted average will be higher than one of the error of $angle'$ and $angle''$. 2) The weighted average can not offset the simultaneous system errors of $angle'$ and $angle''$ since the sum of the coefficient equals to 1. Eq.7 allow us to correct errors in any direction.

The alternative error correction Net combines the errors of $angle'$ and $angle''$ complementarity through Eq.7 to reduce both of them. The accuracy and reliability of an estimated angle ($angle_{EST}$) is reflected by its absolute error ($\|angle_{EST} - angle_0\|$) and relative error ($\|angle_{EST} - angle_0\|/\|angle_{EST}\|$), respectively. The alternative error correction Net uses a norm-angle ($angle_{norm}$) to normalize local relative error, which shows the local characteristics of a loss function to learning the error descenting direction, and an angle sequence ($angle[n]$)to show the effect of absolute error, which shows the descending step of the loss function.

3) NORM-ANGLE BASED ON LOCAL RELATIVE ERROR

Considering $f_{angle^i}(|angle^i - angle_0|)$ is a smooth and monotonous fuction for the absolute error $|angle^i - angle_0|$ of $angle^i$ $(i = 1 or 2)$ (which changes a little in its neightborhood), we formulate the norm-angle as

$$angle^i_{norm} = \frac{angle_0 - angle^i}{\sum_{r=0}^{5^0} l(angle_k) f_{angle^i}(|angle_k - angle_0|) + \epsilon} \tag{8}$$

Here, $angle_k$ are the elements of the input angle set $angle^i$, $r = |angle_k - angle^i|$ is the radius of the neighborhod, ϵ is a small constant avoiding zero denominators. $l(angle_k)$ is the length of the neighborhood of $angle_k$.

$$l(angle_k) = \frac{1}{2}(min(angle|angle > angle_k) - max(angle|angle < angle_k)) \tag{9}$$

Then, we can update the estimation of norm-angle $angle_{est}$ by calculating

$$angle_{est} = argmin(\lambda_{est} norm^1 + (1 - \lambda_{est}) norm^2) \tag{10}$$

where

$$norm^i = \frac{angle - angle^i}{\sum_{r=0}^{5^0} l(angle_k) f_{angle^i}(|angle_k - angle|) + \epsilon} \tag{11}$$

The optimization of $angle_{norm}$ corrects the descent direction, which accerelates the convergence. The initial of angle sequence $angle[0] = (angle', angle'')$.

4) ANGLE SEQUENCE OPTIMIZATION WITH NORM-ANGLE

Expand the $f_{angle^i}(|angle^i - angle_0|)$ in this power series expansion of $x = |angle^i - angle_0|$.

$$\begin{aligned} f_{angle^i}(x) &= f_{angle^i}(0) + f'_{angle^i}(0) * x + o(x^2) \\ &= f'_{angle^i}(0) * x + o(x^2) \end{aligned} \tag{12}$$

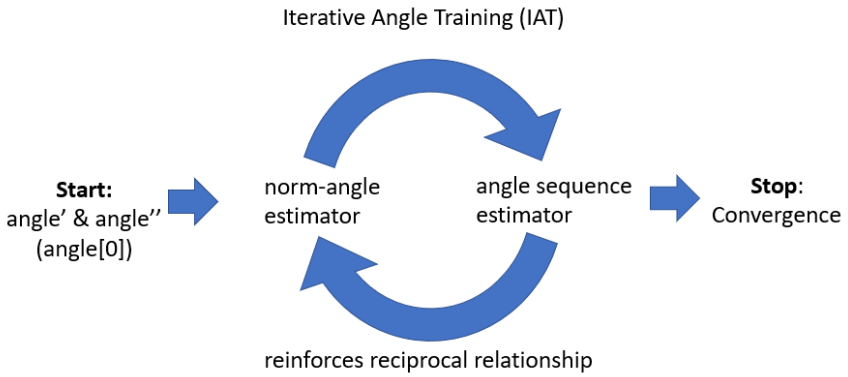

FIGURE 4. The iterative angle training algorithm (IAT) optimizes the norm-angle estimator and angle sequence estimator in tandem for each training batch during training such that the reciprocal relationship between norm-angle and angles is reinforced.

Approximately, norm angle can be defined as

$$angle^i_{norm} = \lambda |angle_0 - angle^i| + \epsilon^i \tag{13}$$

where $\lambda = f'_{angle^i}(0)$. ϵ^i is proportional to $o(angle_0 - angle^i)$ and since it's an infinitesimal quantity, $angle_0$ can be expressed approximately as

$$angle_0 = angle^i + k(angle^i) * angle_{norm}(angle^i) \tag{14}$$

If there is only one estimation, then $angle^i$ is the best approximation of $angle_0$. In our case, we have two inputs

$$angle_0 = angle' + k(angle') * angle_{norm}(angle') \tag{15}$$
$$angle_0 = angle'' + k(angle'') * angle_{norm}(angle'') \tag{16}$$

As Fig. 5 shown, we can combine Eqs. 15 and 16 get a new estimation $angle_{cor}$, we use $angle_{cor}$ instead of one of the $angle'$ and $angle''$ then repeat the optimization. Each new element in the angle sequence has the lowest absolute error in each iteration, which shows the descending step of the loss function. The optimization of angle sequence can improve the accuracy of the estimation.

5) PROPOSED ESTIMATION

Our proposed estimation $angle_{cor}$ has higher order accuracy compared with the estimations of $angle'$ and $angle''$. Subtracting Eq. 15 from Eq. 16, we can have

$$\begin{aligned} &angle' + k(angle') * angle_{norm}(angle') \\ &\quad = angle'' + k(angle'') * angle_{norm}(angle'') \end{aligned} \tag{17}$$

Replace $angle_{norm}$ by Eq. 13, and consider $\epsilon(i) = 0$

$$\begin{aligned} &angle' + K(angle') * |angle_0 - angle'| \\ &\quad = angle'' + K(angle'') * |angle_0 - angle''| \end{aligned} \tag{18}$$

where

$$K(angle^i) = k(angle^i) * \lambda \tag{19}$$

Hence, we have

$$\begin{aligned} angle_{cor} &= angle_0 \\ &= \frac{K(angle'') * angle' - K(angle') * angle''}{K(angle'') - K(angle')} \\ &\quad - \frac{K(angle'') * K(angle')(angle'' - angle')}{K(angle'') - K(angle')} \end{aligned} \tag{20}$$

when $angle'$ and $angle''$ are greater than or less than $angle_0$ at the same time, and a very similar expression for $angle_0$ is between $angle'$ and $angle''$.

In this estimation, we have

$$|angle_0 - angle^i| = |k(angle^i) * angle_{norm}(angle^i)| \tag{21}$$

as a higher order estimation compared with $angle^i$ since here we made a more specific estimation of the error. Actually, for most of the time, $k(angle^i) * angle_{norm}(angle^i)$ is less than $2|angle^i - angle_0|$ unless $|angle' - angle_0|$ and $|angle'' - angle_0|$ different greatly.

III. RESULTS AND ANALYSIS

AEC-Net is validated on the spinal X-ray dataset with signs of scoliosis of varying extents. Extensive experiments show that our method with significant effectiveness, which can be practically used in clinical scoliosis analysis.

A. DATA AND IMPLEMENTATION DETAILS

Our dataset consists of 581 spinal anteriorposterior x-ray images provided by local clinicians. All the images used for training and testing show signs of scoliosis to varying extents. Since the cervical vertebrae (vertebrae of the neck) are seldom involved in spinal deformity, we selected 17 vertebrae composed of the thoracic and lumbar spine for spinal shape characterization. Each vertebra is located by four landmarks with respect to four corners thus resulting in 68 points and 3 Cobb angles per spinal image. These landmarks and the Cobb angles were manually annotated by two professional experienced experts in London spine center based on

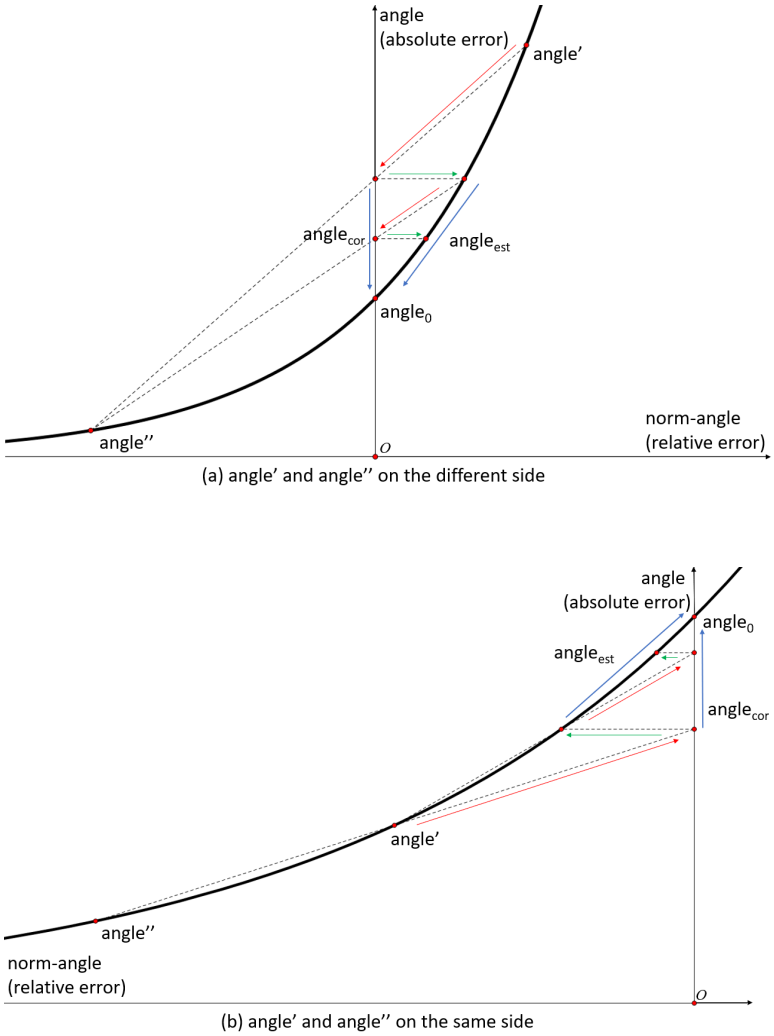

FIGURE 5. The optimization of alternative error correction net. Using high-precision calculation, iteratively optimize the norm-angle (red arrows) and angle sequences (green arrows) to approach the ground truth. For ground truth $angle_0$ and two angles $angle'$ and $angle''$, the proof shows the improvement using linear estimation for the angle accuracy and shows the accuracy of our method.

visual cues. This procedure relies on clinicians to identify the most tilted vertebrae endplates on the x-ray images [3] and then measuring the Cobb angles between those vertebrae. During training, the pixel coordinates were scaled based on original image dimensions such that the range of values lies between 0-256(row) or 0-128(column) depending on where the pixel coordinates lie with respect to the original image (e.g. (128, 64) is the exact centre of the image). We then divided our data according to 481 training set (trainset) and 100 testing set (testset) such that no patient is placed in both sets. We then trained and validated our model on the trainset and tested the trained model on the testset. Since DL methods like our AEC-Net typically require large amounts of training data, we augmented our data in order teach our network the various invariance properties in our dataset. The types of augmentation used include: 1) Adding Gaussian Noise directly to our image in order to simulate inherent noise and 2) Randomly adjusting the brightness and contrast in order to learn the appearance characteristics of the image.

TABLE 3. Accuracy of landmark net, angle net, and AEC-Net.

Method	MAE(degree)	SMAPE(%)
Landmark Net	13.85	38.87
Angle Net	9.36	23.91
AEC-Net	4.90	23.59

B. TEST RESULTS

As shown in Table 3, our model achieved an average mean absolute error (MAE) of 4.90° in Cobb angle detection and achieved a symmetric mean absolute percent error (SMAPE) of 23.59% based on 481 images and is demonstrated as an accurate method. After training each of the models listed in

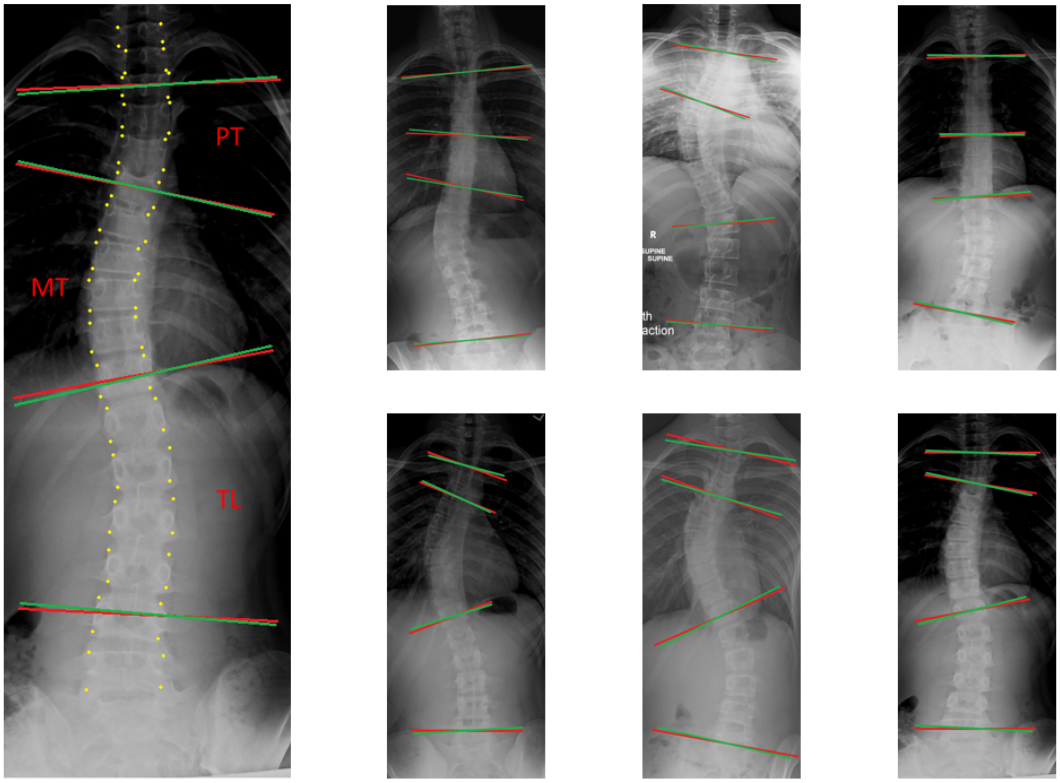

FIGURE 6. The results of cobb angles estimation using AEC-Net. The red lines are ground truth, and the green lines are our test performance. The yellow dots are landmarks.

the table 3 on all 481 images from the trainset, we evaluated each model on the testset consisting of 100 unseen images. The accuracy of AEC-Net has about 8.95° MAE improvement compared with Landmark Net, it also has about 4.46° MAE improvement compared with Angle Net. The lowest error of our AEC-Net base on the improvement on the previous Nets indicates AEC-Net has higher accuracy. Fig. 6 shows the Cobb angle estimation using the AEC-Net compared with the ground truth. It overcomes huge variations and high ambiguities and achieves high accuracy in Cobb angles detection.

Compared with other methods, our model has achieved more effective results. As shown in Table 4, we compare with three other methods, (i.e. support vector regression (SVR) [7], shape regression machine (SRM) [18] and structured support vector regression (S^2VR) [16] the relative root mean squared error (RRMSE) and the correlation coefficient, which shows the accuracy of our method. Our method achieves the lowest average RRMSE of 11.88%, which shows it is superior to other methods. In the robust test, we add Gaussian noise $i\sigma$ to the images. Experiments show our AEC-Net is still valid after adding noise and it's robust.

The correlations between the estimated angles and ground truth are depicted in Fig. 7. The proposed method achieves a correlation coefficient of 0.903, 0.906, 0.945 for the PT, MT and TL angles, which shows the prediction of our AEC-Net has high consistency with ground truth.

TABLE 4. The comparison of the average RRMSE against different methods. Average: The average of landmark net and angle net, AEC-Net + $i\sigma$ noise: The AEC-Net with a gaussian noise of $i\sigma$.

Method	RRMSE (%)
SVR [7]	23.72
SRM [18]	23.35
S^2VR [16]	21.63
Landmark Net	19.40
Angle Net	12.18
Average	13.20
AEC-Net	11.88
AEC-Net + 1σ noise	11.96
AEC-Net + 2σ noise	12.62
AEC-Net + 3σ noise	13.76
AEC-Net + 4σ noise	16.93
AEC-Net + 5σ noise	21.28

C. ANALYSIS

The AEC-Net achieved the lowest average mean absolute error of 4.90° and symmetric mean absolute percent error of 23.59% on the unseen testset. This is due to the contributions of (1) the rough estimation methods (Landmark Net and Angle Net), which successfully learned boundary and spine curve feature embedding as it is the basement for the accuracy of the algorithm and (2) the alternative error correction Net, which faithfully corrects the Cobb angle error of Landmark Net and Angle Net. The success of our method

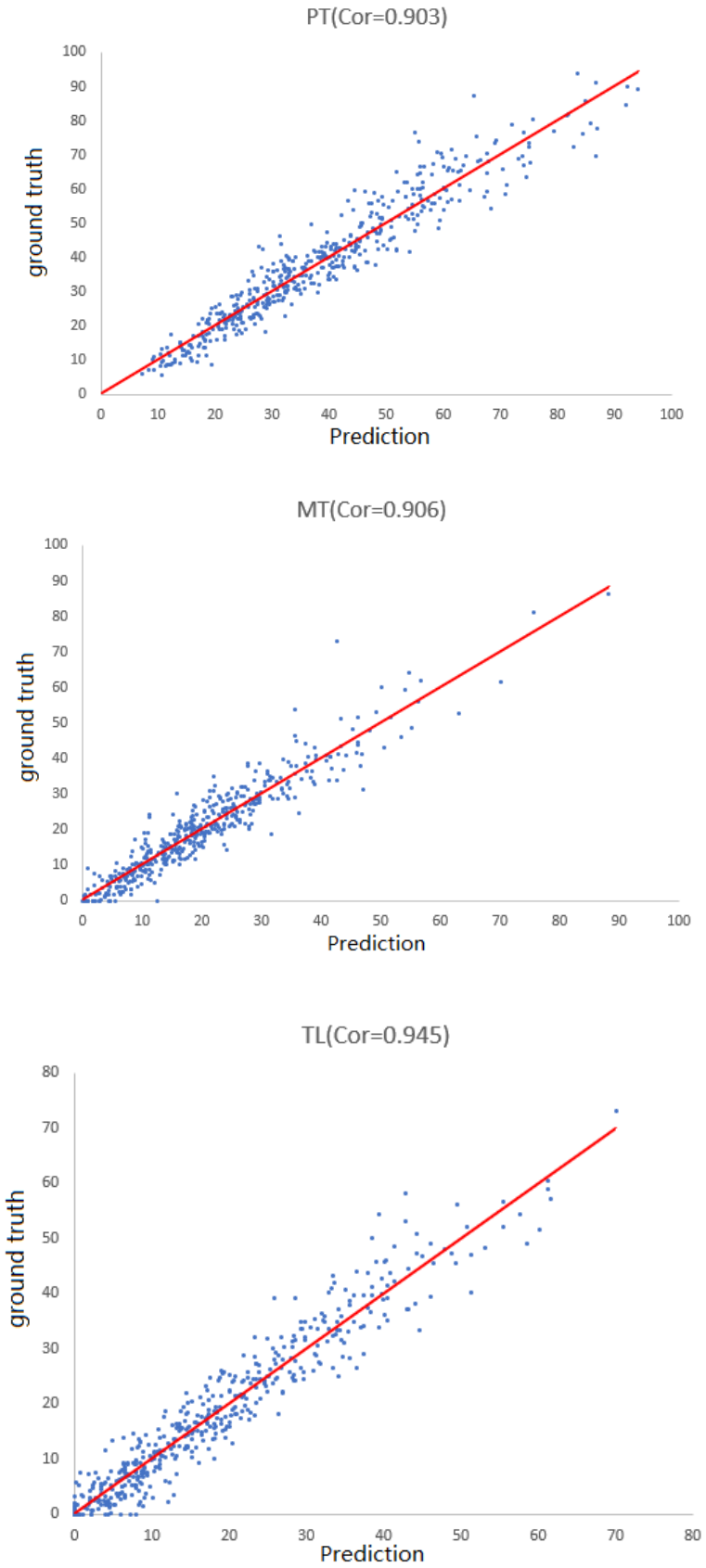

FIGURE 7. The correlations between estimated angles and ground truth.

is further exemplified by the more than 3 degree on average of mean error as well as more rapid convergence compared to the conventional Landmark Net and Angle Net deep learning model. Because of the extrapolation effectively estimate the errors of two initial results and offset their errors each other, the combination of two angles based on extrapolation leads to a lower error. Since the two initial estimations achieved a satisfactory accuracy to a certain extent, our AEC-Net achieves a significant improvement.

IV. CONCLUSION

We have proposed a novel spinal Cobb angle estimation framework that uses our newly designed Adaptive Error Correction Net architecture to assess Cobb angle measurement automatically. The proposed Adaptive Error Correction Net consists of nonlinear mapping and explicit structure modelling, which can handle the highly non-linear relationship between image features and quantitative evaluation parameters and explicitly learn the circular output corrections. Moreover, the alternative error correction Net corrects the error of the Landmark Net and Angle Net. The highly accurate Cobb angles produced by our framework can not only be used by clinicians for comprehensive scoliosis assessment but can also be further extended to other clinical applications.

ACKNOWLEDGMENT

(Bo Chen and Qiuhao Xu contributed equally to this work.)

REFERENCES

[1] S. L. Weinstein, L. A. Dolan, J. C. Y. Cheng, A. Danielsson, and J. A. Morcuende, "Adolescent idiopathic scoliosis," *Lancet*, vol. 371, no. 9623, pp. 1527–1537, 2008.

[2] K. A. Greiner, "Adolescent idiopathic scoliosis: Radiologic decision-making," *Amer. Family Physician*, vol. 65, no. 9, pp. 1817–1822, May 2002.

[3] T. Vrtovec, F. Pernuš, and B. Likar, "A review of methods for quantitative evaluation of spinal curvature," *Eur. Spine J.*, vol. 18, no. 5, pp. 593–607, May 2009.

[4] H. Anitha and G. K. Prabhu, "Automatic quantification of spinal curvature in scoliotic radiograph using image processing," *J. Med. Syst.*, vol. 36, no. 3, pp. 1943–1951, Jun. 2012.

[5] H. Anitha A. K. Karunakar, and K. V. N. Dinesh, "Automatic extraction of vertebral endplates from scoliotic radiographs using customized filter," *Biomed. Eng. Lett.*, vol. 4, no. 2, pp. 158–165, Jun. 2014.

[6] T. A. Sardjono, M. H. F. Wilkinson, A. G. Veldhuizen, P. M. van Ooijen, K. E. Purnama, and G. J. Verkerke, "Automatic cobb angle determination from radiographic images," *Spine*, vol. 38, no. 20, pp. 1256–1262, Sep. 2013.

[7] M. Sánchez-Fernández, M. de Prado-Cumplido, J. Arenas-García, and F. Pérez-Cruz, "SVM multiregression for nonlinear channel estimation in multiple-input multiple-output systems," *IEEE Trans. Signal Process.*, vol. 52, no. 8, pp. 2298–2307, Aug. 2004.

[8] H. Wu, C. Bailey, P. Rasoulinejad, and S. Li, "Automatic landmark estimation for adolescent idiopathic scoliosis assessment using BoostNet," in *Proc. Int. Conf. Med. Image Comput. Comput.-Assist. Intervent.*, in (Lecture Notes in Computer Science), vol. 10433. Quebec City, Montorial, QC, Canada, Springer, Sep. 2017, pp. 127–135.

[9] M. Afshin, I. B. Ayed, K. Punithakumar, M. Law, A. Islam, A. Goela, T. Peters, and S. Li, "Regional assessment of cardiac left ventricular myocardial function via MRI statistical features," *IEEE Trans. Med. Imag.*, vol. 33, no. 2, pp. 481–494, Feb. 2014.

[10] M. Afshin, I. B. Ayed, A. Islam, A. Goela, T. M. Peters, and S. Li, "Global assessment of cardiac function using image statistics in MRI," in *Proc. Int. Conf. Med. Image Comput. Comput.-Assist. Intervent.*, 2012, pp. 535–543.

[11] H. Wang, W. Shi, W. Bai, A. M. Simoes M. de Marvao, T. J. W. Dawes, D. P. O'Regan, P. Edwards, S. Cook, and D. Rueckert, "Prediction of clinical information from cardiac MRI using manifold learning," in *Proc. Int. Conf. Funct. Imag. Modeling Heart*, Jun. 2015, pp. 91–98.

[12] Z. Wang, M. B. Salah, B. Gu, A. Islam, A. Goela, and S. Li, "Direct estimation of cardiac biventricular volumes with an adapted Bayesian formulation," *IEEE Trans. Biomed. Eng.*, vol. 61, no. 4, pp. 1251–1260, Apr. 2014.

[13] X. Zhen, A. Islam, M. Bhaduri, I. Chan, and S. Li, "Direct and simultaneous four-chamber volume estimation by multi-output regression," in *Proc. Int. Conf. Med. Image Comput. Comput.-Assist. Intervent.*, 2015, pp. 669–676.

[14] X. Zhen, Z. Wang, A. Islam, M. Bhaduri, I. Chan, and S. Li, "Direct estimation of cardiac Bi-ventricular volumes with regression forests," in *Proc. Int. Conf. Med. Image Comput. Comput.-Assist. Intervent.*, 2014, pp. 586–593.

[15] X. Zhen, Z. Wang, A. Islam, M. Bhaduri, I. Chan, and S. Li, "Multi-scale deep networks and regression forests for direct bi-ventricular volume estimation, " *Med. Image Anal.*, vol. 30, pp. 120–129, May 2016.

[16] H. Sun, X. Zhen, C. Bailey, P. Rasoulinejad, Y. Yin, and S. Li, "Direct estimation of spinal Cobb angles by structured multi-output regression," in *Proc. Int. Conf Inf. Process. Med. Imag.*, in (Lecture Notes in Computer Science), vol. 10265. Boone, NC, USA, Springer, 2017, pp. 529–540.

[17] A. Quarteroni, R. Sacco, and F. Saleri, *Numerical Mathematics*, 2nd ed. Heidelberg Germany: Springer, 2010.

[18] S. K. Zhou, "Shape regression machine and efficient segmentation of left ventricle endocardium from 2D B-mode echocardiogram," *Med. Image Anal.*, vol. 14, no. 4, pp. 563–581, Aug. 2010.

BO CHEN received the Ph.D. degree from McMaster University, Canada, in 2006. For the past ten years, she was a Research Scientist with Canada Headquartered International Corporation (Alcohol Countermeasure Systems). She joined the Digital Imaging Group of London, Western University, in 2018. Her current interest is the advanced deep learning methods for medical imaging.

QIUHAO XU, photograph and biography not available at the time of publication.

LIANSHENG WANG, photograph and biography not available at the time of publication.

STEPHANIE LEUNG, photograph and biography not available at the time of publication.

JONATHAN CHUNG, photograph and biography not available at the time of publication.

SHUO LI received the Ph.D. degree in computer science from Concordia University, Montreal, QC, Canada, in 2006. He is currently an Adjunct Research Professor with Western University and an Adjunct Scientist with the Lawson Health Research Institute. He is also leading the Digital Imaging Group of London, Western University, as the Scientific Director. His current research interest includes automated medial image analysis and visualization.